F. Lifetimes

1. *From VC-NMD and Gamma-NMD*

As an alternative to the VC-ALD models for predicting phonon lifetimes (Section), we use the normal mode decomposition (NMD) method.[37,38] NMD maps the atomic trajectories (positions and velocities) of atoms in an MD simulation onto the vibrational normal mode coordinates,(cite)

$$q(^{\kappa}_{\nu};t) = \sum_{\alpha,b,l}^{3,n,N} \sqrt{\frac{m_b}{N}} u_\alpha(^{l}_{b};t)\, e^*(^{\kappa\ b}_{\nu\ \alpha}) \exp[i\boldsymbol{\kappa}\cdot \mathbf{r}_0(^{l}_{0})] \tag{9}$$

and

$$\dot{q}(^{\kappa}_{\nu};t) = \sum_{\alpha,b,l}^{3,n,N} \sqrt{\frac{m_b}{N}} \dot{u}_\alpha(^{l}_{b};t)\, e^*(^{\kappa\ b}_{\nu\ \alpha}) \exp[i\boldsymbol{\kappa}\cdot \mathbf{r}_0(^{l}_{0})]. \tag{10}$$

where $\mathbf{r}_0(^{l}_{0})$ are the equilibrium positions of the atoms in the lth unit cell of the lattice supercell under the VC approximation. (needs work) The total energy of a given mode is given by

$$E(^{\kappa}_{\nu};t) = \frac{\omega(^{\kappa}_{\nu})}{2} q(^{\kappa}_{\nu};t)^*\, q(^{\kappa}_{\nu};t) + \frac{1}{2} \dot{q}(^{\kappa}_{\nu};t)^*\, \dot{q}(^{\kappa}_{\nu};t). \tag{11}$$

The MD simulation is performed using the perfect and disordered supercells (Section, Fig.). The NMD is performed using the frequencies and eigenvectors from both the VC ($\omega(^{\kappa}_{\nu})$, $e(^{\kappa\ b}_{\nu\ \alpha})$) and the Gamma supercell ($\omega(^{\kappa}_{\nu})$, $e(^{\kappa\ b}_{\nu\ \alpha})$ with κ = [000], Section). The vibrational mode frequencies and eigenvectors are necessary for the mapping of the atomic trajectories from the MD simulation onto the vibrational normal mode coordinates, $q(^{\kappa}_{\nu};t)$ and $\dot{q}(^{\kappa}_{\nu};t)$, which are required to calculate the kinetic, potential, and total ($E(^{\kappa}_{\nu})(t)$) vibrational normal mode energies.(cite) The effects of disorder enter through the trajectories from these MD simulations, which are also used for the GK method (Section).

The normal mode lifetime is predicted using

$$\tau(^{\kappa}_{\nu}) = \int_0^{\infty} \frac{< E(^{\kappa}_{\nu};t)\, E(^{\kappa}_{\nu};0) >}{< E(^{\kappa}_{\nu};0)\, E(^{\kappa}_{\nu};0) >} dt, \tag{12}$$

where the indefinite integral is replaced by a finite integration given the specifications of the MD simulation. This method for predicting the mode lifetime is more robust than other

a bit more detail. not enough context for this comment to make sense

methods for the disordered systems studied in this work (see Appendix B). It does, however, make it more difficult to predict a phonon frequency, so we use the VC predicted frequency for all VC-NMD predictions, which allow for easier comparison to VC-ALD (Section).

For what system?

The lifetimes predicted using VC-NMD and Gamma-NMD are shown in Fig. ~~First,~~ the range of frequencies of the modes for VC-NMD and Gamma-NMD differ ~~slightly, particularly at high frequency,~~ which is due to ~~the~~ difference in the DOS (Fig.). For small intervals of frequency, there are a wider range of predicted lifetimes for Gamma-NMD. This is because there is no symmetry averaging of the mode properties, which is possible for true ~~performed for the modes of VC-NMD given that a~~ VC ~~is assumed.~~(cite)

remove refs to A-D, compare tx to Γ! which one is "correct"?

Lifetimes predicted by both VC-NMD and Gamma-NMD show scalings ~~with frequency which are~~ predicted by the perturbative methods of VC-ALD (Section), in particular scalings of ω^{-2}, ω^{-4} and even faster scaling due to the DOS behavior (Fig. , Section). What is not predicted by the perturbative VC-ALD methods is the behavior at the highest frequencies, where τ *constant*, which is seen roughly for both VC-NMD and Gamma-NMD, except at $c = 0.5$ for VC-NMD. In general, the lifetimes predicted by both VC-NMD and Gamma-NMD are larger than the Ioffe-Regel (IR) limit,[39]

do you need to discuss tx-tx0 here? Focus on tx vs. Γ you will compare to ad later

$$\tau = 2\pi/\omega. \qquad \frac{2\pi}{\omega} \qquad (13)$$

The physical interpretation of the IR limit is that of a mode ~~which~~ that scatters in a time less than its oscillation period, which is satisfied for most modes in Fig. At the highest frequencies, the existence of this characteristic (thought not exactly minimum) lifetime for LJ argon is analagous to the minimum mean free path used in a simple models of glasses.[40] There is, however, no theoretical prediction of this high-frequency behavior.

22 not satisfied for most modes

it's not really clear what you are talking about - make better use of fig. to motivate this important discussion

While it is possible to predict a MFP given the VC predicted group velocities and the lifetimes predicted by VC-NMD, we find that it is not useful to understanding this high-frequency beavhior. For the group velocities predicted from the VC dispersion, they generally trend towards 0 as the wavevector is increased to the BZ boundaries. This would predict a MFP of 0, which is not helpful to the current discussion. Furthermore, the concept of a MFP becomes poorly defined the more the system is disordered (e.g. dilute alloys to high concentration and amorphous phases). It is thus more useful to consider the proposed lower-limit of the mode thermal diffusivities, which combine the mode lifetime and effective group velocity, or equivalenty, effective MFP (Section).

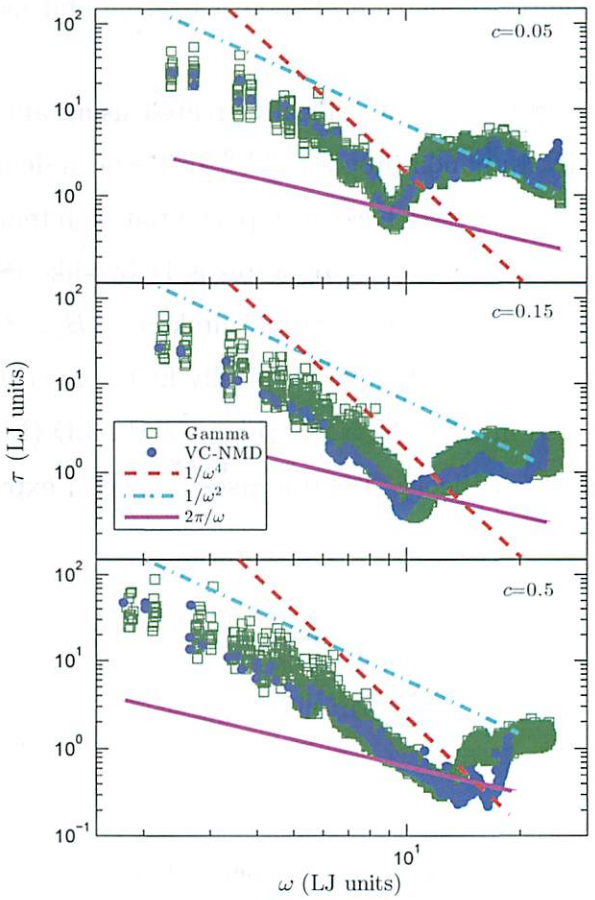

FIG. 4: Lifetimes predicted using VC-NMD and Gamma NMD from MD simulations of mass disordered lattice supercells (Section). Both ω^{-2} and ω^{-4} scalings can be observed at low frequencies, which are predicted by the peturbative models used for VC-ALD (Section). For both VC-NMD and Gamma NMD, most mode lifetimes are greater than the Ioffe-Regel limit $\tau = 2\pi/\omega$.[39] While there is more "noise" in the Gamma mode data (Section), the lifetime magnitudes and trends agree well, an important consideration when comparing VC-NMD and VC-ALD in Fig. .

2. From VC-ALD

Assuming initrinsic and disorder scattering mechanisms to operate independently, the effective phonon lifetime can be found using Matthiessen's rule(cite),

$$\frac{1}{\tau(\kappa_\nu)} = \frac{1}{\tau_{p-p}(\kappa_\nu)} + \frac{1}{\tau_d(\kappa_\nu)}, \tag{14}$$

where $\tau_{p-p}(\kappa\nu)$ accounts for intrinsic phonon-phonon scattering and $\tau_d(\kappa\nu)$ accounts for defect scattering.

Phonon-phonon scattering ($\tau_{p-p}(\kappa\nu)$) is typically treated using anharmonic perturbation theory (ALD) including only 3-phonon processes.[1,4,38] It has been demonstrated that the effects of higher order phonon processes become important at high temperatures (see Section).[38,41] At low frequencies where the density of states is Debye-like (~~Section~~ Fig.), $\tau_{p-p}(\kappa\nu)$ follows a scaling due to both normal ($B_1\omega^{-2}$) and umklapp ($B_2\omega^{-2}$) 3-phonon scattering processes, where the constants B_1 and B_2 are typically fit to experimental data.(cite) The scaling $\tau\ \omega^{-2}$ can be observed in both the NMD (Fig.) and ALD (Fig.) predicted results.

Using harmonic perturbation theory, Tamura ~~gives~~ derives a general expression for mass point defect scattering[11]

$$\frac{1}{\tau_d(\kappa\nu)} = \frac{\pi}{2N}\omega^2(\kappa\nu)\sum_{\kappa'\nu'}\delta(\omega(\kappa\nu)-\omega(\kappa'\nu')) \sum_b g_2(b)|e^*(\kappa'\nu' b\alpha)\cdot e(\kappa\nu b\alpha)|^2, \quad (15)$$

where

$$g_n(b) = \sum_\mu c^\mu(b)(1-m^\mu(b)/\bar{m}(b))^n, \quad (16)$$

N is the number of unit cells, and c^μ is the concentration, $m^\mu(b)$ is the mass of the μ-th species and $\bar{m}^\mu$ is the average mass. For the binary LJ argon and SW silicon alloys considered, there is one atom type in the unit cell with $\mu = a, b$, so that the alloying atom labeled by m^b_{1-c} can be considered to be an "isotope" of atom labeled m^a_c. This convention is appropriate because of the perturbative approach used to derive Eq. , while we consider large disorder up to $c = 0.5$.[11]

The term $g_2(b)$ is a coupling term ~~which~~ defines the strength of the disorder which depends on the concentration and masses of the different species. (Give values of g for LJ and SW, at all c = they are approimxately the same given the similar mass ratios used, so that the underprediction of VC-ALD for LJ argon is because of the nature of the system.)

needs work above

Bond disorder can be accounted for using a similar expression with an average atomic radius or suitable scattering cross-section.[42,43] The effect of bond and mass disorder has been investigated computationally by Skye and Schelling for Si/Ge[44], where it was shown that

mass disorder is the dominant scattering mechanism. In this work we consider only mass disorder.

By considering the symmetry properties of the FCC lattices considered in this work (Section), it can be shown that

$$1/\tau_d(\overset{\kappa}{\nu}) = \frac{\pi}{2} g_2 \omega^2(\overset{\kappa}{\nu})\, D(\omega(\overset{\kappa}{\nu})),$$

I think this equation is sufficient, Eqs. (15), (16), (17) not needed

where $D(\omega(\overset{\kappa}{\nu}))$ is the density of states (Section).[11] Under the Debye-approximation ($D(\omega(\overset{\kappa}{\nu}))\ \omega(\overset{\kappa}{\nu})^2$), the phonon scattering due to mass point-defects is given by $A\omega^{-4}$, where A is a constant related to the unit cell volume, branch-averaged group velocity, and disorder coupling strength ($g_2(b)$ in Eq. above). The frequency dependence (ω^4) is the same as Rayleigh scattering, which is valid at low frequency and observed in both the NMD (Fig.) and ALD (Fig.) predicted results. The disorder scattering scaling is expected to fall off faster than ω^{-4} when $D(\omega(\overset{\kappa}{\nu}))$ grows faster than the Debye scaling of ω^2 (Fig. , Section). The lifetimes do fall off faster ω^{-4} for the mass disordered LJ FCC supercells for a narrow range of frequencies near $\omega = 10$ in Fig. for $c = 0.05, 0.15$, but seem to follow more closely ω^{-4} for $c = 0.5$.

try not to mix method with results

For the VC-ALD method, the intrinsic $\tau(\overset{\kappa}{\nu})_{p-p}$ is calculated using the method described in[38], using all classical expressions to remain consistent with the classical MD-based methods NMD and GK (Section). To calculate the disordered lifetimes $\tau(\overset{\kappa}{\nu})_d$ (Eq.), it is necessary to broaden the δ function using a Lorentzian function.[1] footnote[1] For all calculations, the Lorentzian was broadened using a value of $100\delta_{\omega,avg}$ (Section). For the system sizes here, the results do not differ significantly if this broadening value is varied manually or by increasing system size (N_0).

Higher-order terms in the Tamura theory can be represented by terms involving g_n (where $b = 1$, Eq. (Eq)) and $I(\omega)$, defined as

$$I(\omega) = \frac{1}{6N} \sum_{(\overset{\kappa}{\nu})} \frac{\omega(\overset{\kappa}{\nu})^2}{\omega(\overset{\kappa}{\nu})^2 - \omega - i\epsilon}, \tag{18}$$

where ϵ is a small number, taken to be $100\delta_{\omega,avg}$. For example, the predicted frequency shifts due to disorder scattering are

$$\delta\omega/\omega = g_2(b) Re[I(\omega)]/2, \tag{19}$$

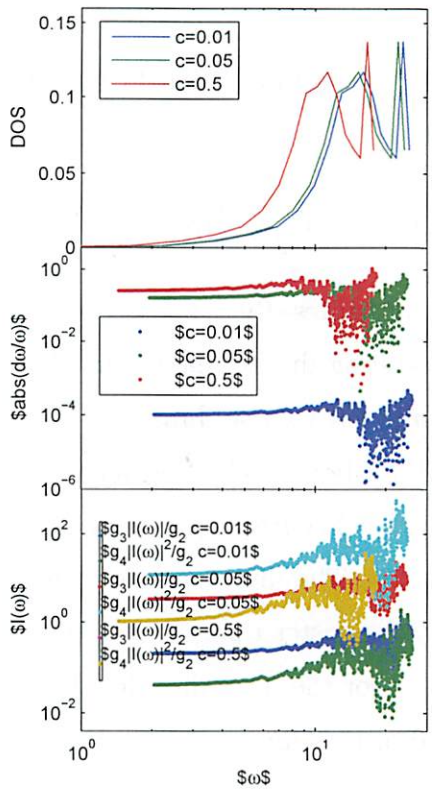

not needed

FIG. 5: lj tamura results

and the terms $g_n|I(\omega)|^{n-2}/g_{n-1}$ represent estimates for the higher-order terms of the defect-perturbed phonon self-enegy (linewidth), which are shown in Fig (Fig).[11] In the original study of isotope scattering in Ge, the perturbation was small and the higher-order terms were shown to be negligible. In the present study, which includes large amounts of disorder (*e.g.* large values of g_n), the predicted frequency shifts and higher-order estimates are not small, especially at high frequency. The effect of these higher-order terms is important to understanding the results predicted by VC-ALD in Section and Section .

quantity at order of magnitude level

G. Diffusivities

not Pauli

In the classical harmonic limit, where the specific heat $c_p(\kappa_\nu) = k_B$, a vibrational mode's contribution to thermal conductivity is determined by the mode thermal diffusivity. For phonons, the thermal diffusivity is

$|\vec{v}_g(\kappa)|^2$

$$D_{ph}(\kappa_\nu) = \boldsymbol{v}_g^2(\kappa_\nu)\,\tau(\kappa_\nu)\,. \tag{20}$$

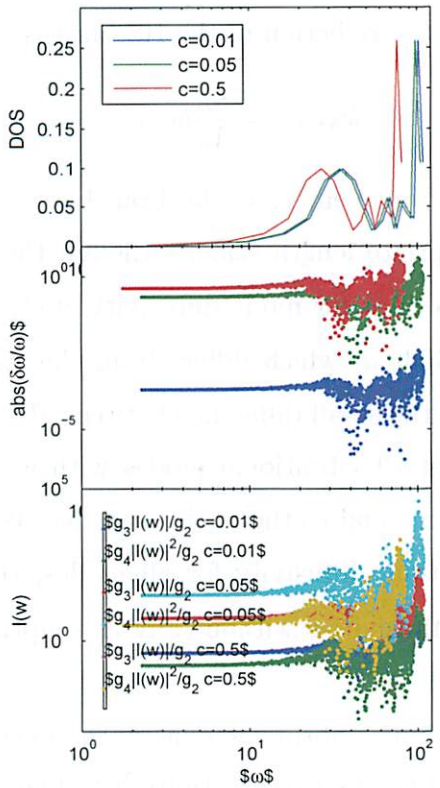

not needed

FIG. 6: sw tamura results

Here, $\boldsymbol{v}_g^2(\substack{\kappa \\ \nu})$ is calculated from the VC dispersion (Section) for both VC-NMD and VC-ALD, so any differences in thermal diffusivity comes from the difference in the lifetimes predicted by these two methods. meaning what?

In explicitly disordered systems, modes can transport heat by harmonic coupling due to disorder in the Allen-Feldman (AF) theory of diffusons.[16] The AF theory predicts the mode-specific thermal diffusivity of disordered vibrations. In the AF theory, the mode diffusivities typically diverges as $\omega \to 0$ because the vibrational modes are long-wavelength plane waves (phonons) that weakly scattered by the disorder.[45,46] footnote[] (For the disordered lattices studied in this work for $c \leq 0.15$, the predicted k_{AF} is strongly system size dependent, indicating this diverging behavior. For $c = 0.5$, the divergence with system size is small for the range of system size studied ($N_0 = 4$ to $N_0 = 12$), where $k_{AF}/k_{GK} = 0.93$ for $N_0 = 12$.)

In the high-scatter (HS) limit,(cite) the AF diffusivity of each mode is

rightarrow

$$D_{AF,HS} = \frac{1}{3} v_s a, \tag{21}$$

make links to all Figures

pick one of CP or HS - is there any need for both?

and the AF thermal conductivity prediction in the HS limit is

$$k_{AF,HS} = \frac{k_B}{V_b} b v_s a, \tag{22}$$

where V_b is the volume of the unit cell, v_s is the branch-averaged sound speed, and a is the lattice constant (or appropriate length scale, although the choice of this length scale is not unique.).[31] A similar HS limit for mode diffusivity is given by the Cahill-Pohl (CP) HS model,(cite) $D_{CP,HS} = 0.403 v_s a$, which differs from the AF,HS model by a factor of approximately %20.[31] Ignoring the small difference between the AF,HS and CP,HS models, the physical interpretation is of all vibrational modes with a group velocity equal to the sound speed and mean-free path equal to the lattice spacing. While the CP,HS and AF,HS models assume a constant thermal diffusivity for all modes, the AF theory is capable of predicting the mode specific diffusivities without any assumptions other than a harmonic approximation.(cite)

provided there are no propagating modes

With sufficient disorder, such as amorphous phases, the harmonic AF theory is capable of accurately predicting a finite thermal conductivity.[22,47] The thermal conductivity of the LJ amorphous phase (with an effective mass of 2) is predicted by the AF theory, $k_{AF} = 0.099 W/m = K$. footnote[] (The amorphous LJ phase was created by liquifying the crystal and instantly quenching by removing all kinetic energy. The resulting structure was then energy minimized and annealed in an NPT ensemble at zero pressure and $T = 10$ K.(cite lammps)) The mode-specific thermal diffusivities for the LJ argon amorphous phase are shown in Fig. 5, where modes with significant contribution to thermal transport can be modeled using a mode-independent diffusivity of approximately $D_{AF,HS}$ (Eq.). Also shown are the AF predicted thermal diffusivities for the explicitly disordered superlattice and $c = 0.5$.

details of amorphous phase should be introduced earlier

While the AF theory is divergent in the low-frequency limit for lattices, the finite system size bounds the thermal diffusivities of the lowest frequencies (Fig), and the thermal conductivity predicted by the AF theory is actually quite close to that predicted by the GK method, $k_{AF}/k_{GK} = 0.93$. More importantly, the thermal diffusivity of all modes in the explicitly disordered lattice supercell are finite, except at the highest frequencies where they tend to 0 as in the amorphous phase (Fig). This places a plausible lower-bound on the value of the VC phonon mode diffusivities, $D_{ph} \geq D_{AF,HS}$. In fact, the thermal properties of disordered lattices and glasses has been explained heuristically by assuming that phonons

are scattered so strongly by structural disorder that transport becomes diffusive, with a frequency regime of small, constant thermal diffusivity.[48,49]

The lower-limit of the thermal diffusivity predicted for the VC modes is $D_{ph}(\overset{\kappa}{\nu}) \approx 0$, as is the case for the VC mode MFP because of the VC predicted group velocities (Section). In typical explicitly disordered system, this lower limit of the thermal diffusivity is only seen for a minority of modes at the highest frequencies, which is true for the disordered LJ systems shown in Fig. Feldman et al showed that the thermal diffusivities in a-Si show a sharp breakpoint at the on- set of localized states, where it tends to zero exponentially. Similar behavior is seen for the LJ argon disordered superlattices and amorphous phase ($c = 0.5$, Fig.).

meaning what?

For both VC-NMD and VC-ALD, a significant number of modes have $D_{ph}(\iota;t)\, D_{AF,HS}$ (Fig.). This can lead to an underprediction of the total thermal conducitvity. The diffusivity of these modes can be adjusted such that any mode with $D_{ph}(\iota;t)\, D_{AF,HS}$ is given $D_{ph} = D_{AF,HS}$. The result of this adjustment, referred to as VC-NMD* and VC-ALD*, is examined in the thermal conductivity predictions in Section.

For LJ argon, VC-NMD predicts lifetimes which are generally larger than the period ($\tau(\overset{\kappa}{\nu}) > 2\pi/\omega(\overset{\kappa}{\nu})$) of the vibrational oscillation (Ioffe-Regel limit)(cite), and actually increase then remain approximately constant at high frequency (Section and Fig.). VC-ALD predicts essentially monotonically decreasing lifetimes with increasing frequency for both LJ argon and SW silicon (Fig.). Because VC-NMD and VC-ALD use the same values for $v_g(\overset{\kappa}{\nu})$, the phonon mode diffusivities $D_{ph}(\overset{\kappa}{\nu})$ are also underpredicted for VC-ALD compared to VC-NMD. There are thus 2 underpredictions to consider when predicting the thermal conductivities in Section : underprediction of the thermal diffusivity assuming the VC phonon modes for VC-NMD and VC-ALD, and the underprediction of the mode lifetimes by the VC-ALD perturbative models. OK

not used, yet...

energy transport in jammed sphere packings[50] heat transport in model jammed solids[46]

II. THERMAL CONDUCTIVITY PREDICTIONS

The thermal conductivity can be predicted using the mode properties predicted by the VC-NMD and VC-ALD methods. However, given the discussion of the mode properties

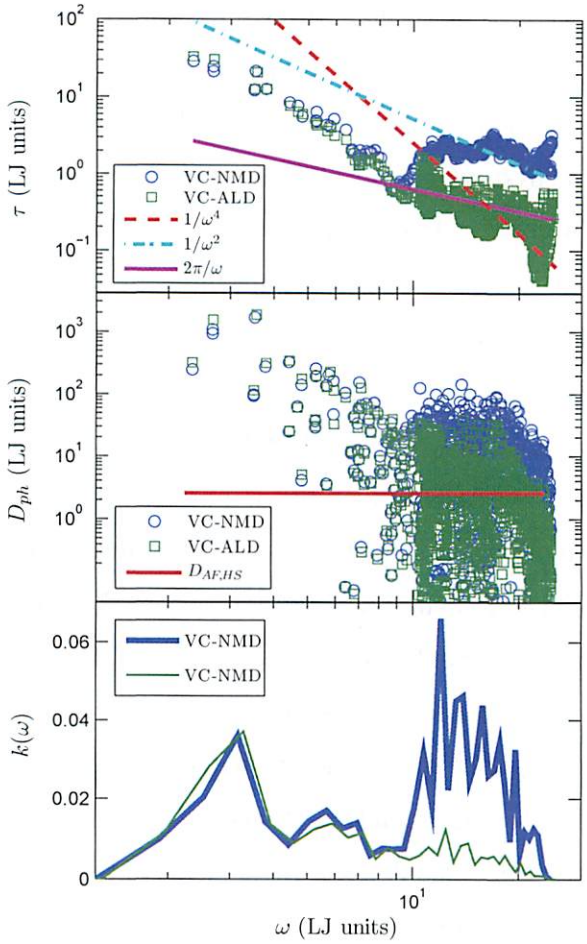

FIG. 7: (a) predicted lifetimes for VC modes using VC-NMD and VC-AlD for LJ argon. (b) predicted VC mode thermal diffusivities, compared to the AF,HS limit. (c) the thermal conducitivty frequency spectrum, which is peaked at high frequency, in contrast to SW silicon (Fig).

preceeding this section, it is necessary to implement a third method for predicting thermal condudctivity. We choose the equilibirum MD-based green-Kubo (GK) method. This method does not predict any mode-specific properties, and is thus a system-level prediction. For this reason, thermal conductivity predicted by GK has been shown to capture the effects of whatever scattering meachanisms are present in the MD simulation without any other assumptions (other than those which come with the classical nature of the MD siulation).(cite) Details of the GK and MD simulations are given in Appendix.

For LJ argon, bulk thermal conductivity predictions are made for VC-NMD, VC-ALD

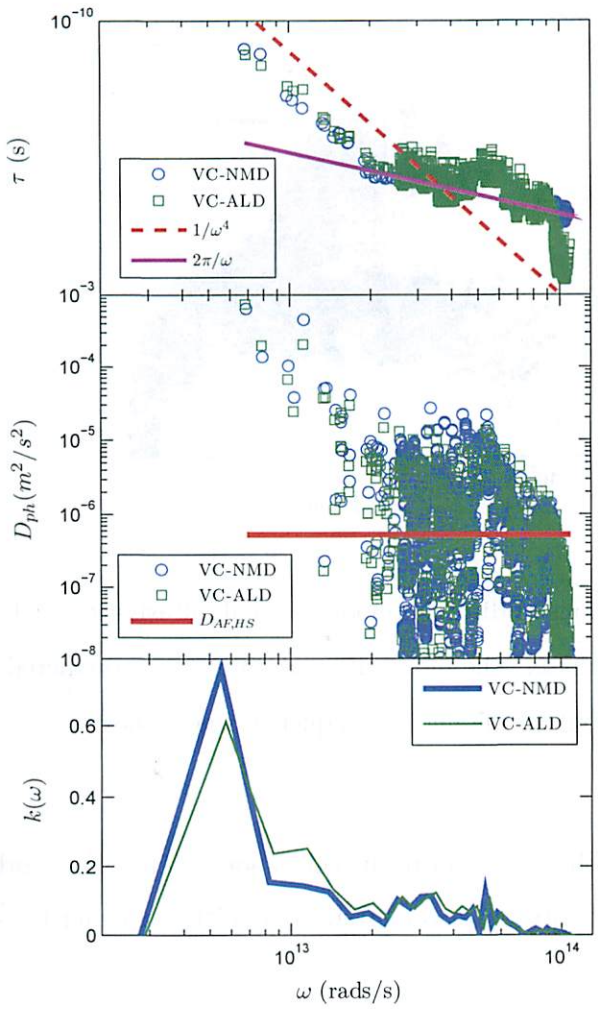

FIG. 8: (a) predicted lifetimes for VC modes using VC-NMD and VC-AlD for SW silicon. (b) predicted VC mode thermal diffusivities, compared to the AF,HS limit. (c) the thermal conducitivty frequency spectrum, which is peaked at low frequency, in contrast to LJ argon (Fig).

First mention (I think) motivate!!

and GK (Fig.). For SW silicon, bulk thermal conductivity predictions can only be made for VC-ALD and GK because of the limited system size used for VC-NMD (see Appendix). For LJ argon, both VC-NMD and VC-ALD underpredict the thermal conductivity compared to GK.

From Fig. it is clear that both VC-NMD and VC-ALD underpredcit compared to GK. The underprediction is only modest for VC-NMD, on the order of 20% or less for all c. By adjusting the mode diffusivity as suggested in Section , the thermal conductivtiy predicted by VC-NMD* is brought into agreement with GK by approximately 10% or less for all c.

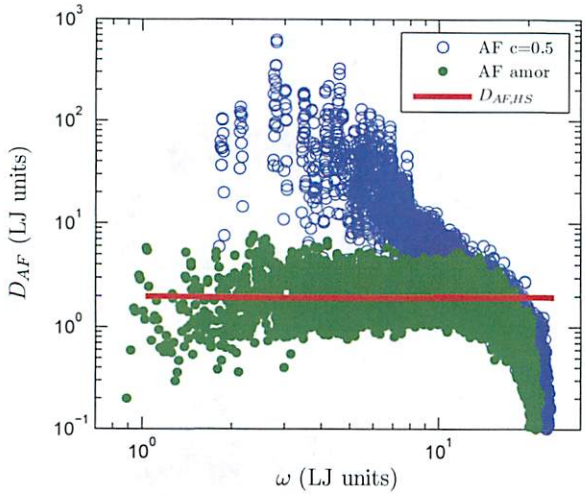

FIG. 9: AF theory predictions of disorded mode thermal diffusivities for LJ argon disorded lattice supercell and amorphous phase. The mode thermal diffusivities predicted for the disorded lattice supercell are all finite, except at the highest frequency where they tend to 0 as in the amorphous phase.

When combined with the high-scatter limit, this suggests that the mode properties predicted by VC-NMD are a fair representation of the explicitly disorderd modes used in the MD simulation.

The VC-ALD method underpredicts the thermal conductivity for all c, where the underprediction is worst at $c = 0.5$ where $k_{VC-ALD}/k_{GK} = 0.56$ and is well outside the error bars of the calculations (which are on the order of the large symbol sizes in Fig.). By applying the high-scatter limit adjustment VC-ALD*, the thermal conductivities are brought into marginally better agreement, worst for $c = 0.05$ where $k_{VC-ALD^*}/k_{GK} = 0.65$. This is because of the underprediction of the mode lifetimes at high frequency for VC-ALD compared to VC-NMD in Section , since the two methods share the same mode group velocities.

The failure of the VC-ALD method can be demonstrated further by moving to higher temerpature ($T = 40$ K Fig.). The beginning breakdown of the intrinsic scattering model ($\tau_{p-p}(\overset{\kappa}{\omega})$) can be observed for the perfect ($c = 0.0$) crystal at $T = 40$ K (see Fig.), where ALD begins to overpredict compared to GK. This can be explained by the emerging importance of higher order (n> 3) n-phonon process at high temperatures.[38] While the VC-ALD method begins to overpredict at this elevated temperature, it continues to underpredict for the alloys

what about the Tp-d model, higher-order? terms?